Published in final edited form as:
J Control Release. 2014 October 10; 191: 24–33. doi:10.1016/j.jconrel.2014.03.041.

Neutral Polymer Micelle Carriers with pH-Responsive, Endosome-Releasing Activity Modulate Antigen Trafficking to Enhance CD8 T-Cell Responses

Salka Keller[a], **John T Wilson**[a], **Gabriela I Patilea**[a], **Hanna B Kern**[a], **Anthony J Convertine**[a], and **Patrick S Stayton**[a]

Salka Keller: salka@uw.edu; John T Wilson: wilsonjt@uw.edu; Gabriela I Patilea: patilg@uw.edu; Hanna B Kern: kernh@uw.edu; Anthony J Convertine: aconv@uw.edu; Patrick S Stayton: stayton@uw.edu

[a]Department of Bioengineering, Box 355061, University of Washington, Seattle, WA 98195-1721, USA

Abstract

Synthetic subunit vaccines need to induce $CD8^+$ cytotoxic T-cell (CTL) responses for effective vaccination against intracellular pathogens. Most subunit vaccines primarily generate humoral immune responses, with a weaker than desired $CD8^+$ cytotoxic T-cell response. Here, a neutral, pH-responsive polymer micelle carrier that alters intracellular antigen trafficking was shown to enhance $CD8^+$ T-cell responses with a correlated increase in cytosolic delivery and a decrease in exocytosis. Polymer diblock carriers consisted of a *N*-(2-hydroxypropyl) methacrylamide corona block with pendant pyridyl disulfide groups for reversible conjugation of thiolated ovalbumin, and a tercopolymer ampholytic core-forming block composed of propylacrylic acid (PAA), dimethylaminoethyl methacrylate (DMAEMA), and butyl methacrylate (BMA). The diblock copolymers self-assembled into 25–30 nm diameter micellar nanoparticles. Conjugation of ovalbumin to the micelles significantly enhanced antigen cross-presentation *in vitro* relative to free ovalbumin, an unconjugated physical mixture of ovalbumin and polymer, and a non pH-responsive micelle-ovalbumin control. Mechanistic studies in a murine dendritic cell line (DC2.4) demonstrated micelle-mediated enhancements in intracellular antigen retention and cytosolic antigen accumulation. Approximately 90% of initially internalized ovalbumin-conjugated micelles were retained in cells after 1.5 h, compared to only ~40% for controls. Furthermore, cells dosed with conjugates displayed 67-fold higher cytosolic antigen levels relative to soluble ovalbumin 4 h post uptake. *S*ubcutaneous immunization of mice with ovalbumin-polymer conjugates significantly enhanced antigen-specific $CD8^+$ T cell responses (0.4 % IFN-γ^+ of $CD8^+$) compared

Corresponding Author: Patrick S. Stayton, Box 355061, Department of Bioengineering, University of Washington, Seattle, WA 98195, Tel: 1-206-685-8148, stayton@uw.edu.

Conflict of interest statement

Dr. Stayton is a co-founder of PhaseRx Inc. that has licensed some of the polymer technology represented in this work from the University of Washington. All work described in this report was conducted at the University of Washington independently of PhaseRx Inc. and supported as described in the Acknowledgements.

to immunization with soluble protein, ovalbumin and polymer mixture, and the control micelle without endosome-releasing activity. Additionally, pH-responsive carrier facilitated antigen delivery to antigen presenting cells in the draining lymph nodes. As early as 90 min post injection ova-micelle conjugates were associated with 28% and 55% of dendritic cells and macrophages, respectively. After 24 h, conjugates preferentially associated with dendritic cells, affording 30-, 3-, and 3-fold enhancements in uptake relative to free protein, physical mixture, and the non pH-responsive conjugate controls, respectively. These results demonstrate the potential of pH-responsive polymeric micelles for use in vaccine applications that rely on $CD8^+$ T cell activation.

Keywords

polymer micelles; pH-responsive; nanoparticles; subunit vaccine; CD8 T cell response

1. Introduction

Protein subunit vaccines present a safer alternative to live and inactivated vaccine vectors, but there is a general need for delivery vehicles that induce a more potent, antigen-specific $CD8^+$ cytotoxic T-cell (CTL) response against intracellular pathogens like HIV, malaria, and tuberculosis [1–4]. Induction of such a response requires antigen presentation via class I major histocompatibility complex (MHC-I) by dendritic cells. Exogenous antigens are endocytosed by antigen presenting cells and degraded into peptides within compartments of the endo/lysosomal processing pathway. Peptides generated in these compartments are predominantly presented on the cell surface via MHC-II complexes, giving rise to $CD4^+$ T-cell responses [2,3]. Some specialized subsets of dendritic cells can cross-present exogenous antigens to MHC-I via a variety of intracellular pathways, yet CTL stimulation is often minimal [3]. Directing extracellular antigen to the cell cytoplasm for processing via the classical cross-presentation pathway is one approach to promote MHC-I restricted antigen presentation for CTL activation [4,5].

Considerable research has focused on the development of particle-based, synthetic delivery systems in the viral size range (~20–200 nm) [2,6,7] that can protect antigen against degradation [8], enhance cross-presentation [9,10], and facilitate uptake by professional antigen presenting cells (APCs) [14–16]. These include liposomes [12,13], immune stimulating complexes (ISCOMs) [3], and polymer-based nanoparticles such as polymerosomes [14,15], dendrimers [11,16], and micelles [9,10]. Our group has previously reported on polymeric antigen carriers that incorporate pH-dependent, endosomal releasing activity [17–19]. This polymer activity mimics that of some viruses which have evolved to evade lysosomal degradation through the activity of fusogenic coat proteins that undergo a pH-induced conformational change to a membrane destabilizing state [20].

Recently, we described the reversible addition-fragmentation chain transfer (RAFT)-based synthesis of a new type of amphiphilic diblock carrier for RNA therapeutics that self-assembles into 25–30 nm micelles under physiological conditions (pH 7.4) [18]. These carriers are composed of a neutral hydrophilic *N*-(2-hydroxypropyl) methacrylamide (HPMA) [21] corona featuring pyridyl disulfide (PDS) functionalities for the conjugation of biologic drugs, and a previously exploited pH-responsive endosomal-releasing core

containing dimethylaminoethyl methacrylate (DMAEMA), propylacrylic acid (PAA), and butyl methacrylate (BMA) [19,22]. The neutral corona imparts micelles with a favorable toxicity profile over cationic carriers, and we have shown that the PDS moieties can reversibly link to a variety of thiolated cargo [4,18]. The latter is especially attractive for antigen delivery, as Hirosue *et al* and Nembrini *et al* have also shown that bond reversibility under reducing conditions is associated with enhanced cross-presentation [23,24].

In this study, we demonstrate that antigen conjugation to this micelle carrier promotes antigen uptake and accumulation in the cytosol of murine dendritic cells (DC 2.4), reduces exocytosis, and enhances cross-presentation. We further show that protein-polymer conjugates preferentially associate with DCs in the draining lymph node. Immunization with conjugates elicited antigen-specific $CD8^+$ T cell and antibody responses in the absence of any additional vaccine adjuvant, demonstrating the potential of this delivery platform for protein- based vaccine applications.

2. Materials and Methods

Materials

Chemicals and reagents were purchased from Sigma-Aldrich and used as received unless otherwise specified. 4,4′-Azobis(4-cyano valeric acid) (V501) was purchased from Wako Chemicals USA, Inc. Trithiocarbonate CTA, ethyl cyanovaleric trithiocarbonate (ECT) [22], pyridyl disulfide methacrylamide (PDSMA) [25], and propylacrylic acid (PAA) [26] were synthesized as previously reported. HPMA was purchased from Polysciences, Inc. Butyl methacrylate (BMA) was passed through a short column of basic alumina and poly(dimethylaminoethyl methacrylate) (DMAEMA) and methacrylic acid (MMA) were distilled prior to use. Bond-Breaker TCEP solution, Traut's reagent (2-iminothiolane-HCl), Ellman's reagent (5,5′-dithio-bis-[2-nitrobenzoic acid]; DTNB), and HALT protease inhibitor cocktail were obtained from Thermo Scientific. ^{3}H-N-Succinimidyl propionate was purchased from American Radiolabeled Chemicals. Antibodies for intracellular cytokine staining were purchased from BD Bioscience.

Polymer Synthesis

Poly(HPMA-*co*-PDSMA)-*b*-(PAA-*co*-DMAEMA-*co*-BMA) was synthesized as previously described with minor modifications [18]. The macroCTA *poly*(HPMA-*co*-PDSMA) was prepared in a mixed solvent system of ultra-pure water/ethanol (2:1 vol:vol) at 70°C under a nitrogen atmosphere for 4–5 h. ECT and V501 were used as chain transfer agent (CTA) and radical initiator, respectively. The initial CTA to monomer molar ratio ($[CTA]_0$:$[M]_0$) was 200:1, and the initial CTA to initiator molar ratio ($[CTA]_0$:$[I]_0$) was 10:1. A PDSMA concentration of 8% was targeted. HPMA was dissolved in molecular grade water (Hyclone) and immediately added to CTA and PDSMA dissolved in ethanol for a final concentration of 16 wt. % monomer and macroCTA to solvent. Lastly, initiator was added from a stock solution in ethanol. Post polymerization ultra-pure water was added to the reaction solution. The solution was frozen under liquid nitrogen and water removed by lyophilization for 48 h. The resultant polymer was dissolved in methanol and precipitated (4X) in an excess of ether. Residual ether was removed by a final precipitation with pentane followed by drying *in*

vacuo overnight. For addition of the second block, macroCTA dissolved in dimethyl acetamide (DMAc) was added to PAA, DMAEMA and BMA to obtain a final concentration of 30 wt. % monomer and macroCTA to solvent. The initial molar feed ratio of PAA:BMA:DMAEMA was 3:4:3. $[M]_0/[CTA]_0$ and $[CTA]_0/[I]_0$ were 500:1 and 2.5:1, respectively. Following addition of V70, the solution was purged with nitrogen for 30 min and reacted for 18 h at 30°C. The resulting diblock copolymer was purified by precipitation (4X) from methanol into an excess of pentane/ether (3:1 vol:vol). The final precipitant was rinsed with pentane and dried under vacuum overnight. The polymer was re-dissolved at 200 mg/mL in MeOH, dripped into an excess of ultra-pure water, and lyophilized. *Poly*(HPMA)-*b*-(PAA-*co*-DMAEMA-*co*-BMA) was synthesized in the same manner, with the exception of no PDSMA monomer in the first block. *Poly*[(HPMA-*co*-PDSMA)-*b*-(MMA)] non pH-responsive control polymer was prepared by chain extension of the *poly*[(HPMA-*co*-PDSMA) macroCTA described here with methyl methacrylate (MMA) according to the protocol described by Lundy *et al* [18].

Polymer Characterization

Absolute molecular weights and polydispersities (PDI) were determined by gel permeation chromatography (GPC) as described previously [9]. Polymer compositions were determined by ^{1}H-NMR (Bruker AV500) in deuterated methanol (CD_3OD) at 25°C. Reduction of the diblock polymer in the presence of Bond-Breaker TCEP solution (~210 molar excess per polymer) followed by spectroscopic measurement of the liberated pyridine-2-thione (ε_{343} = 8080 $M^{-1}cm^{-1}$) after 1 h was used as a secondary method for quantifying incorporation and retention of PDSMA. Additional synthetic details, summaries of polymer properties, representative NMR spectra and GPC traces can be found in the Supplementary Information.

Formulation of Polymer Micelles

From their lyophilized form, polymers were reconstituted to induce micelle formation as described previously [9]. Briefly, polymer was dissolved at 50 mg/mL in EtOH and dripped into 1X PBS (0.0067 M PO_4, pH 7.2, HyClone) to obtain a final polymer concentration of 10 mg/mL. Ethanol was removed by 4 rounds of buffer exchange into 1X PBS using Amicon Ultra-0.5 mL Centrifugal Filters (3K MWCO). Final ethanol content was < 1% as determined using an Amplite ethanol quantitation kit according to the manufacturer's instructions. Polymer concentration post ethanol removal was determined spectrophotometrically via absorbance of the aromatic PDS groups at 284 nm or, for the non-PDS containing polymer, the trithiocarbonate chain ends at 312 nm. Prior to use, polymer micelles were sterilized using 0.22 μm syringe filters (Pall Corporation).

Formation of Protein-Polymer Conjugates

For all studies, an average of 4 thiol residues were introduced onto the model antigen ovalbumin (45 kDa). A 22 molar excess of 2-iminothiolane (Traut's reagent) was added to a 10 mg/mL solution of the protein in sodium phosphate buffer (100 mM, pH 8.0, 1 mM EDTA). The reaction was mixed continuously on a rotator for 1 h at RT. Unreacted Traut's reagent was removed using a Zeba desalting column (0.5 mL, 7K MWCO, Thermo Scientific) equilibrated with 1X PBS (HyClone). The degree of thiol modification was

determined using Ellman's reagent as described by the manufacturer. For the preparation of fluorescent conjugates, ovalbumin was labeled with an amine reactive dye, AlexaFluor488-TFP (Invitrogen) prior to thiolation (~0.5–1 dye/protein) according to the manufacturer's instructions. Thiol-functionalized protein solutions were filter-sterilized, and subsequently reacted with polymer micelles (prepared as described above) at a polymer to protein molar ratio of 20:1 at RT overnight under sterile conditions. Extent of conjugation was verified by non-reducing SDS-polyacrylamide gel electrophoresis (SDS-PAGE) using conjugates prepared with fluorescently-labeled ova [9]. To show reducibility of the disulfide bond between the polymer and protein, conjugates were incubated with 20 mM Bond-Breaker TCEP solution for 1 h prior to running the gel.

Static and Dynamic Light Scattering

Static and dynamic light scattering measurements were conducted using a Malvern Zetasizer Nano ZS (Worcestershire, UK) at a constant scattering angle of 173° as described previously [9]. Briefly, particle sizes of diblock copolymer micelles and protein-polymer conjugates were determined by dynamic light scattering (DLS) at RT in 1X PBS (pH 7.4) at 1 mg/mL polymer. In some cases, DLS measurements were performed with copolymers (1 mg/mL) incubated with 100 mM sodium phosphate buffer (supplemented with 150 mM NaCl) in the pH range of the endosomal processing pathway (7.4, 7.0, 6.6, 6.2, and 5.8). Mean diameters are reported as the number average ± standard deviation from three or more independently prepared formulations. Micelle molecular weight ($M_{w,micelle}$) and second virial coefficient (A_2) were estimated from Debye plots based on the d*n*/d*c* of the micelle solution as measured using an Optilab-rEX refractometer (Wyatt). Micelle aggregation number (N_{agg}) was determined based on the relationship $N_{agg} = M_{w,micelle}/M_{w,unimer}$.

Red Blood Cell Lysis

The capacity of free polymer and protein-polymer conjugate to promote pH-dependent disruption of lipid bilayer membranes was assessed via a red blood cell hemolysis assay as previously described [27]. Briefly, polymer or conjugate were incubated for 1 h at 37°C in the presence of human erythrocytes at 40 μg/mL in 100 mM sodium phosphate buffer (supplemented with 150 mM NaCl) in the pH range of the endosomal processing pathway (7.4, 7.0, 6.6, 6.2, and 5.8). Extent of cell lysis (i.e. hemolytic activity) was determined spectrophotometrically by measuring the amount of hemoglobin released (A_{541} nm). Hemolytic activity was normalized to a 100% lysis control (1% Triton X-100 treated red blood cells). Samples were run in triplicate.

Cell Lines

DC 2.4s (H-2K^b-positive murine dendritic cell line) were generously provided by K. Rock (University of Massachusetts Medical School). Cells were cultured in RPMI 1640 (Gibco) medium supplemented with 10% fetal bovine serum (FBS, PAA Laboratories or Gibco), 100 U/mL penicillin/100 μg/mL streptomycin (GIBCO), 2 mM L-glutamine, 55 μM 2-mercaptoethanol (Gibco), 1X non-essential amino acids (Cellgro) and 10 mM HEPES (Invitrogen). Cells were passaged at ~60–70% confluency using 0.25% trypsin-EDTA (Gibco). B3Z T cells, a lacZ-inducible T cell hybridoma specific for SINFEKL complexed

with H-2K^b, were kindly provided by N. Shastri (UC Berkeley) and cultured in RPMI 1640 (Gibco) supplemented with 10% FBS, 100 U/mL penicillin/100 μg/mL streptomycin (GIBCO), 2 mM L-glutamine, 55 μM 2-mercaptoethanol (Gibco), and 1 mM sodium pyruvate (Gibco). All cell lines were grown at 37°C and 5% CO_2.

In vitro Cytotoxicity

Diblock copolymer toxicity was evaluated in DC2.4 cells using a CellTiter 96AQueous One Solution Cell Proliferation Assay (MTS, Promega Corp). Cells were plated in 96-well plates (10,000 cells/well) and allowed to adhere overnight. Media was aspirated and replaced with 200 μL of fresh media containing polymer or conjugate at the appropriate concentrations. Samples were run in sextuplicate and cytotoxicity determined after 4 or 24 h using using the CellTiter assay according to manufacturer's protocols. Absorbance measurements (A_{490} nm) were obtained using a Tecan Safire 2 microplate reader. Reported values were normalized to untreated cells.

In vitro MHC-I Antigen Presentation

The polymer's ability to promote antigen presentation to MHC-I was evaluated by a lacZ antigen presentation assay [4,9,11]. A specialized *Lac*Z B3Z CTL hybridoma which produces β-galactosidase upon binding ovalbumin class I antigenic epitope SINFEKL complexed with MHC-I H-2K^b present on DC2.4s, acts as a reporter cell to determine the degree to which ovalbumin is presented as a class I antigen [28]. DC2.4s were cultured overnight (50K cells/well) in 96-well U-bottom plates (BD Falcon). The following day, samples (10 μL) were added in quadruplicate at a final concentration of 10 or 100 μg/mL ova and allowed to incubate for 4–5 h at 37°C. SINFEKL peptide (0.25 μg/mL) and PBS were used as positive and negative controls, respectively. Post incubation, cells were carefully rinsed 2X with 1X DPBS, and B3Z cells (100K cells/well) were added and co-cultured with DCs for 24 h. Cells were pelleted via centrifugation for 7 min at 1250 rpm, media was carefully aspirated, and cells were resuspended in 150 μL of CPRG/lysis buffer (1X PBS supplemented with 0.15 mM chlorophenol red-β-D-galactopyranoside (CalBiochem), 0.1% Triton-X 100, 9 mM MgCl, 100 μM mercaptoethanol). Plates were incubated at 37°C in the dark for 24 h, at which time 100 μL of sample was transferred to 96-well clear flat-bottom plates and the absorbance of released chlorophenol red measured at 570 nm with a reference at 595 nm using a Tecan Safire 2 plate reader. Reported values are normalized to SINFEKL peptide (0.25 μg/mL).

Preparation of Radiolabeled Polymer and Conjugates

To determine the dynamics of uptake and exocytosis, conjugates were prepared with tritium-labeled ova. Ova (100 mM sodium phosphate buffer pH 8, 1mM EDTA) was labeled with ^{3}H-N-succinimidyl propionate (DMF) for 2 h in the dark at RT. The reaction was conducted using 2 mg/mL protein, and radiolabel was added such as to obtain 5% vol:vol DMF in the final reaction mixture. Excess radiolabel was removed using two Zeba desalting columns (2 mL, 7K MWCO; Thermo Scientific) equilibrated with pH 8 sodium phosphate buffer. For studying polymer trafficking dynamics, radiolabeled polymer was prepared by reacting ^{3}H-iodoacetamine with tertiary amines on core DMAEMA residues. ^{3}H-

iodoacetamine (1 mCi/ml in EtOH) and polymer (50 mg/ml in EtOH) were combined to a final target concentration of 12.5 μCi/mg polymer, and allowed to react for 1 h at RT in the dark on a rotator. Labeled polymer was assembled into micelles in 1X PBS, and passed through two 2 mL Zeba desalting columns (Thermo Scientific) equilibrated with dH2O to remove unreacted label. The solution was subsequently lyophilized. The specific reactivity of ^{3}H-ova and ^{3}H-polymer were determined using a liquid scintillation counter (Beckman LS6500) with Ultima Gold scintillation fluid (PerkinElmer).

Uptake and Exocytosis of Radiolabeled Ova and Conjugates

For uptake experiments, DC2.4 cells were plated in 24 well plates (BD Falcon) at 100,000 cells/well. Cells were dosed with radiolabeled samples (2.5 μg/ml ova) and allowed to incubate for 4 h. For exocytosis experiments, cells were pulsed for 4 hours with each treatment group upon which media was replaced and cells were further incubated for various chase times. At the end of each chase period, cells were washed once with 1X PBS and lysed with 1X RIPA buffer (Thermo Scientific). Radioactivity of cell lysates was measured using a liquid scintillation counter.

Cellular Fractionation

DC2.4 cells were plated at 6.5×10^{6} cells/plate in 150 mm TC-treated dishes (CellTreat) in 20 ml complete media and allowed to adhere overnight. The following day, cells were dosed with treatment groups (2.5 μg/ml ova) for 4 h, and subsequently chased for various times up to 4 h. At the end of either pulse or chase periods, media was removed and cells were washed once with cold PBS. To collect cells from culture dishes, cells were gently lifted using a flat edge cell scraper and 10 ml cold PBS. Cells were pelleted by centrifugation at 100 *g* for 5 min at 4°C, followed by resuspension in cold 5 mL homogenization buffer (0.25 M sucrose, 10 mM HEPES, 1 mM EDTA, pH 7.4) and another round of centrifugation at 200 *g* for 6 min at 4°C. Pellets were weighed and re-suspended in homogenization buffer (vol = 2.5X pellet weight) supplemented with HALT protease inhibitor (1:100, Thermo Fisher). Cells were homogenized with 30 strokes of a syringe with a 25 gauge needle to achieve 80–90% cell breakage as determined using an LDH cytotoxicity assay kit (Takara). Cells treated with 0.05% Triton-X 100 represented 100% cell breakage. Lysates were centrifuged at 1000 *g* for 10 min at 4°C to sediment nuclei and unbroken cells. The remaining pellet, termed the nuclear pellet (NP), was re-suspended in homogenization buffer supplemented with protease inhibitor. The resulting post-nuclear supernatant (PNS) was further separated into cytosolic (C) and vesicular (V) fractions by ultracentrifugation at 100,000 *g* for 30 min at 4°C. Sample radioactivity was read using a liquid scintillation counter (Beckman) and Ultima Gold scintillation fluid (Perkin-Elmer).

Characterization of Subcellular Fractions

The relative purity of cytosolic and vesicular fractions was assayed as described previously with minor modifications [29]. Briefly, fractions were analyzed for lactate dehydrogenase (cytosol; LDH cytotoxicity kit, Takara) and hexosaminidase A [29] (lysosome) activity, and probed for Rab5 (endosome) and Lamp2 (lysosome) markers using a Western blot. Total protein content was measured using a Bradford-based protein assay kit (Bio-Rad). For

Western blots, 10 μg total protein from cytosolic and vesicular fractions was reduced using 1X Laemmli buffer (BioRad) containing β-mercaptoethanol, and denatured by incubation at 100°C for 10 min. Samples were run by SDS-PAGE as previously described [29] and proteins were transferred onto a PVDF membrane (Bio-Rad) in transfer buffer (12 mM Tris-base, 100 mM glycine, 10% MeOH, 0.1% w/v SDS) for 1.5 h at 100V. Non-specific binding sites were blocked with SuperBlock PBS-Tween 20 (Thermo Scientific) for 1 h at RT. Membrane was incubated with mouse cross-reactive anti-human Rab5 (1:200, SantaCruz Biotech) or rat anti-mouse Lamp2 (1:400; Developmental Studies Hybridoma Bank; DSHB) in blocking buffer for 1 h at RT. After 3X 10 min washes with PBS-Tween 20 (PBST, Sigma-Aldrich), membranes were probed with HRP-conjugated goat anti-mouse antibody (1:50,000; BD Pharmingen) or HRP conjugated anti-rat antibody (1:20,000; Santa Cruz Biotech) in blocking buffer for 1 h at RT. Membranes were washed 3X for 10 min in PBST and incubated with West Femto chemiluminescence substrate (Thermo Scientific) for 5 min. Finally, chemiluminescence was detected using a Kodak Image Station 4000MM and band intensity was calculated using Image J.

Animals

Female C57Bl/6 mice, 6 to 8 weeks old, were purchased from The Jackson Laboratory (Bar Harbor, ME), maintained at the University of Washington under specific pathogen-free conditions and treated in accordance with the regulations and guidelines of the University of Washington Institutional Animal Care and Use Committee.

Lymph Node Biodistribution Studies

To evaluate the distribution of vaccine formulations in the draining lymph nodes, fluorescent conjugates were prepared using AlexaFluor647-carboxylic acid succinimidyl ester (Molecular Probes)-labeled ova (~1.4 dye/protein). Mice were injected with treatment groups (12.5 μg ova, 150 μg polymer) into the dorsal part of the right hind foot (20 μL). Prior to immunization mice were anesthetized with isofluorane. Either 90 min or 24 h post injection mice were sacrificed and the draining popliteal lymph nodes harvested to assess antigen uptake in lymphocyte populations. Lymph nodes from two random mice were pooled to obtain a single data point for each group. Lymph nodes were incubated in digest buffer (RPMI 1640, 2 mM L-glutamine, 0.34 mg/ml Liberase TL (Roche), 2 mg/ml DNaseI (Roche)) for 20 min at 37°C. Post digestion, lymph nodes were mechanically homogenized using a 70 μm cell strainer, washed with 1X PBS, and incubated with cell dissociation solution (Sigma) for 10 min at 37°C. This reaction was quenched with RPMI 1640 media supplemented with 10% heat inactivated FBS (Gibco). Cells were subsequently incubated with lysis buffer (BD Pharm/lyse) at RT for 5 min to lyse red blood cells. The reaction was quenched with 1X PBS and cells were washed, counted, and resuspended in 150 μL stain buffer (BD Pharmingen). Lymphocytes were plated at $2–5\times10^6$ cells/well (150 μL) in 96-well U-bottom plates and incubated with Fc-block (anti-CD16/CD32, BD Bioscience) for 15 min at 4°C. Post incubation cells were washed once with stain buffer and stained with monoclonal antibodies (mAb) Pacific Blue anti-mouse CD11c (BioLegend), PE-Cy7 anti-mouse CD11b (BD Pharmingen), PerCP-Cy5.5 anti-mouse CD45R/B220 (BD Pharmingen), anti-mouse F4/80 antigen PE (eBioscience), and AlexaFluor-488 anti-mouse CD3e (eBioscience) for 30 mins at 4°C. Following another wash, cells were suspended in stain

buffer and counted by flow cytometry using an LSRII cytometer (Becton Dickinson). Splenocytes isolated from a naiive mouse and processed in the same manner were used as compensation controls. Viable cells were gated by forward and side scatter, height and width, and a minimum of 500,000 events acquired for each sample. Samples were analyzed using FlowJo software (Tree Star Inc.).

Immunization Studies

All vaccine formulations were prepared using low endotoxin grade ovalbumin (<0.01 EU/g; EndoGrade, Hyglos GMBH). Endotoxin levels in prepared samples were periodically tested using a Limulus amoebocyte lysate assay kit (Lonza), and consistently found to be less than 5 EU/kg as recommended by the United States Pharmacopoeia [30]. Mice (n = 7–15 per group) were injected subcutaneously (s.c.) at the base of the tail on days 0 and 21 (opposite sides), with treatment groups (100 μg ova and/or ~1.2 mg polymer in 200 μL PBS; 0.5 mg/mL ova, ~6 mg/mL polymer). Conjugates were prepared one day prior to immunization and stored in a sterile environment. The mixture was prepared by combining non-thiolated endo-free ova (100 mM phosphate buffer, pH 8.0, 1mM EDTA) with polymer (1X PBS; 20M excess to protein) within one hour of immunization. One week post boost immunization (day 28) mice were sacrificed and spleens harvested to assess the cellular immune response as described by Wilson *et al* [9].

Intracellular Cytokine Staining (ICS)

Splenocytes were plated at 2×10^6 cells/well (100 μL) in 96-well U-bottom plates and stimulated with $CD8_{257\text{-}264}$ (SINFEKL) peptide (20 μg/mL) or PMA/ionomycin as a positive control (2 μg/mL) for 9 hr at 37°C. A protein transport inhibitor, GolgiPlug (BD Bioscience), was added 1 h post stimulation begin to induce intracellular accumulation of cytokines. Cells were subsequently washed and stained as described by Wilson *et al* [9]. Viable splenocytes were gated by forward and side scatter, height and width, and 1,000,000 events acquired for each sample. Samples were analyzed with FlowJo software (Tree Star, Inc).

Indirect Enzyme-Linked Immunosorbent Assay (ELISA)

Approximately 100 μL of blood were collected from mice via submandibular bleeding one day prior to sacrifice, and sera tested for ova-specific IgG1 and IgG2c as previously described [9]. Briefly, Nunc MaxiSorp plates (Nunc-Thermo Fisher Scientific Inc.) were coated with 5 μg/mL ovalbumin in 1X DPBS overnight at 4°C. Plates were blocked twice with Super Block Blocking Buffer (Thermo Scientific) and sera were added at a 1:50 dilution and subsequent 5-fold serial dilutions in 0.1% BSA/PBS-Tween 20 (PBST) and incubated for 2 h at RT. To determine cutoff values, serum from a naiive mouse was run on each plate. Post incubation plates were washed with PBST and incubated with biotin-conjugated anti-mouse antibodies to IgG1 (BD Pharmingen) or IgG2c (Bethyl Laboratories) at 0.005 μg/mL in 0.1% BSA/PBST for 1 h at RT. Plates were again washed and incubated with SA-HRP (BD Pharmingen) at a 1:20,000 dilution in 0.1% BSA/PBST for 30 min at RT. Following a final round of washes, plates were developed with 100 μL SureBlue Reserve TMB 1 peroxidase substrate (KPL). After 5 min the enzymatic reaction was

quenched with 1 M HCl and plates were read within 30 min at 450 nm using a Tecan Safire 2 microplate reader. Endpoint titers were determined from reciprocal dilutions using a sigmoidal fit in GraphPad Prism 5 (GraphPad Software Inc.) to determine the dilution at which the 450 nm OD value equaled the cutoff value, defined as the average titer of the naiive group + two standard deviations.

Statistical analysis

Standard one-way analysis of variance (ANOVA) was used to test for treatment effects at a significance of $p<0.05$ followed by Tukey post-test for pairwise comparisons among means.

3. Results

3.1 Preparation of protein-polymer conjugates

pH-responsive diblock copolymers were synthesized by RAFT polymerization [31,32] as described previously [18]. Briefly, a *poly*(HPMA-*co*-PDSMA) macroCTA (MW: 11,500 g/mol, PDI: 1.1) was purified and chain-extended with PAA, DMAEMA and BMA (PDB) to obtain the final diblock copolymer (MW: 26,000 g/mol, PDI: 1.8). The macroCTA and diblock displayed unimodal size distributions by GPC, although an increase in the PDI was observed upon addition of the second block (SI Figure 1). This peak broadening can be attributed to the sterically hindered PAA monomer [18,33,34]. The diblock peak showed a clear transition to lower elution volumes indicating successful chain extension. Final copolymer compositions, determined by ^{1}H-NMR spectroscopy (SI Table 1), were similar to those targeted, with 21% PAA, 25% DMAEMA, and 55% BMA in the second block and 7% PDSMA in the first. A TCEP reduction assay was used in conjunction with NMR analysis to calculate final values of 3 and 5 PDS groups per polymer chain, respectively. A micelle molecular weight of 2010 kDa was determined by static light scattering, indicating an aggregation number of ~80 polymer chains per micelle. A control carrier lacking conjugatable PDS moieties was synthesized in a similar manner (SI Table 2 & Figure 3–4). An additional control polymer containing a non pH-responsive and non endosomal-releasing core (methyl methacrylate, MMA) was prepared as described previously [18] (SI Table 3 & Figure 5–6). For clarification purposes, henceforth the pH-responsive or “active” carrier is referred to as “HP-PDB”, the non-conjugatable control carrier as “H-PDB”, and the non pH-responsive or “inactive” carrier as “HP-MMA”.

Dynamic light scattering analysis in PBS (pH 7.4) yielded hydrodynamic diameters of 30 ± 2 nm, indicative of a micellar morphology. A shift in particle size to below 10 nm at pH 5.8 was consistent with micelle dissociation into unimers (Figure 1a). The incorporation of a neutral corona was anticipated to impart favorable biocompatibility to the antigen delivery system. Indeed, high levels of cell viability were observed in DC2.4 dendritic cells after 4 and 24 h at polymer concentrations of up to 125 and 80 μg/mL, respectively (SI Figure 7, 4 h data not shown). All subsequent *in vitro* assays were conducted in these time and/or concentration ranges.

Reactive thiol groups were introduced on ovalbumin via modification of lysine primary amines with 2-iminothiolane (~4 thiols/ova). pH-responsive Ova-(HP-PDB) and non-responsive Ova-(HP-MMA) conjugates were formed via a disulfide exchange reaction with

the PDS functionalities on the carrier. Conjugation efficiency was monitored by non-reducing SDS polyacrylamide gel electrophoresis using conjugates prepared with fluorescently labeled ova (Figure 1b). A shift of the ova band to higher molecular weights accompanied by disappearance of the free protein was used to monitor protein-polymer coupling. Approximately 95% conjugation was achieved at a polymer:protein ratio of 20:1 (~4 ova/micelle). The distribution of ova over a broad range of molecular weights upon conjugation to active carrier reflects polymer polydispersity, as well as variations in the number of conjugation events per ova or polymer chain [9]. By contrast, the lower polydispersity of the HP-MMA (SI Table 3) yields a tight band on the gel upon antigen conjugation. Incubation of conjugates with reducing agent (20 mM TCEP) for 1 h at RT regenerated the free protein band, demonstrating disulfide bond reversibility and protein release. As anticipated, no conjugation was observed in a physical mixture of ova and the control polymer lacking reactive PDS groups [Ova+(H-PDB)] (Figure 1b). Micelles exhibited no significant size change via DLS following antigen conjugation, suggesting minimal particle cross-linking or aggregation.

The carrier's membrane-destabilizing activities were evaluated using an established red blood cell hemolysis assay (Figure 1c). Both the pH-responsive carrier and ovalbumin conjugate exhibited potent hemolytic activity at endosomal pH values. As expected, the non-pH responsive control carrier was inactive across the studied pH range.

3.2 Polymer carrier enhances antigen cross-presentation *in vitro*

A B3Z presentation assay was performed to assess the carrier's ability to activate CTLs through enhanced MHC-I presentation. DC2.4s were pulsed with polymer conjugates, polymer and ova mixture, and free ova, and subsequently co-cultured with B3Z T cells which produce β-galactosidase upon recognition of $Ova_{257\text{-}264}$ (SIINFEKL) complexed with MHC-I. The pH-responsive Ova-(HP-PDB) carrier showed significantly greater T-cell activation than controls (Figure 2). Physical attachment of antigen to the active carrier was necessary for cross-presentation, as the polymer and ova mixture minimally activated CTLs. While observed enhancements in T cell activation may be due to differences in intracellular antigen processing, they could also be a result of varied antigen uptake between species (SI Figure 10a). To minimize the effect of antigen uptake on cross-presentation, Ova and Ova-(HP-MMA) were also dosed at 100 μg/mL ova, a concentration at which uptake was comparable to that of Ova-(HP-PDB) at 10 μg/mL after 4 h (SI Figure 10b). No substantial increase in cross-presentation was observed at this higher antigen dose (Figure 2). These data, along with evidence in our previous work demonstrating a dependence on endosomal acidification in polymer-mediated antigen cross-presentation [9], strongly suggest that the membrane interactive properties of HP-PDB play a key role in facilitating antigen display by MHC-I.

3.3 Polymer carrier potentiates antigen uptake and intracellular retention

To gain insight into the mechanism by which this carrier may be enhancing antigen cross-presentation, a series of cellular fractionation studies was conducted to quantitatively assess ova accumulation in cytosolic and vesicular compartments of DC2.4 cells. Marker enzyme assays for LDH (cytosol) [35] and HexA (lysosomes) [36], and immunoblotting for Rab5

(early endosomes) [37] and Lamp2 (late endosomes and lysosomes) [38] were used to assess fraction purity. The procedure yielded reproducible marker distribution, with a majority of LDH (~80%) and minimal HexA (~20%), Lamp2 (~10%) and Rab5 (~10%) in cytosolic fractions (SI Figure 8). The total amount of antigen in cytosolic fractions after a 4 h pulse followed by various chase periods was determined for free ova and the active conjugate. Immediately after the pulse, total ova levels observed in cytosolic and vesicular fractions were ~10 times higher for cells treated with Ova-(HP-PDB) relative to free protein (Figure 3a and b). While intracellular antigen levels in cells dosed with soluble ova gradually decreased over time, cells dosed with conjugate retained high antigen levels over the 4 h chase period, peaking at 67-fold and 74-fold enhancements over soluble protein in cytosolic and vesicular fractions, respectively. This trend is likely a result of enhanced uptake combined with prolonged intracellular retention mediated by the membrane-interactive polymer segment. Interestingly, the intracellular localization of tritium-labeled HP-PDB polymer was ~90% associated with the vesicular membrane fraction after a 4 h pulse (SI Figure 9), suggesting that the hydrophobic, cationic core partitioned with vesicle-membrane lipids [29] while significant fractions of the ova cargo was released to the cytosol.

A series of pulse-chase experiments was performed to characterize the dynamics of antigen exocytosis. Cells were incubated with radiolabeled samples at an equivalent ova dose for 4 h, and subsequently chased for another 4 h. At each chase time point supernatant was removed, cells were washed and lysed, and the remaining intracellular radioactivity was measured. From this, the amount of ova taken up and respectively exocytosed was calculated as a percentage of the amount internalized after the 4 h pulse. Conjugation to carrier markedly decreased the amount of ova exocytosed compared to control groups (Figure 3c). In fact, at the 15 min timepoint we observed ~30% exocytosis of control groups, as compared to a modest ~7% for Ova-(HP-PDB). After 4 h, the percent of ova exocytosed rose to ~ 40% for conjugate and greater than 80% for controls. Interestingly, in control groups most exocytosis occurred within 15 min, while ova delivered via HP-PDB was predominantly retained within cells for up to 1.5 h. Combined, fractionation and exocytosis studies demonstrate that conjugation to pH-responsive micelles enhances antigen uptake and significantly increases cytosolic delivery as well as endosomal-lysosomal residence times in DC2.4 cells.

3.4 Polymer conjugation facilitates antigen delivery to draining lymph node APCs

Previous studies have shown that sub-100 nm nanoparticles readily transport into lymphatic vessels and subsequently to APCs in draining lymph nodes [7,10,15,39,40]. The transport of the polymeric micelle carriers to draining lymph nodes and delivery to lymphocyte subsets was evaluated using AlexaFluor647-labeled ova. Ninety minutes or 24 h after injection, the draining popliteal lymph nodes were isolated and analyzed by flow cytometry to characterize antigen uptake by lymphocyte subsets. By 90 min post injection, a large percentage of cells (~12%) were ova-positive with HP-PDB (Figure 4a). This percentage decreased to ~3% 24 h post injection (Figure 4b). Significantly lower levels of uptake were observed for control groups at both time points (Figure 4a and b). Injection of Ova-(HP-PDB) afforded a ~2.5-fold increase in dendritic cell uptake and up to ~2.8 fold increase in macrophage uptake relative to controls (Figure 4c). Co-localization of conjugates with

lymph node APCs 90 min post injection is suggestive of primarily passive transport via the draining lymphatics [41,42]. 24 h post injection, ova was exclusively associated with dendritic cells and macrophages (Figure 4d) for all groups. The active carrier enabled superior ova uptake in dendritic cells compared to free protein (30-fold increase), the ova and polymer mixture (3-fold increase), and HP-MMA polymer (3-fold increase), with corresponding ~4-fold, ~2-fold, and ~1.5-fold increases in macrophage uptake, respectively. For a potential vaccine platform, targeting dendritic cells in the lymph nodes is attractive, as these cells are primarily responsible for antigen presentation to and co-stimulation of T-cells. Co-localization of conjugates with lymph node APCs 90 min post injection is suggestive of primarily passive transport via the draining lymphatics [41,42].

3.5 Conjugates enhance antigen-specific $CD8^+$ T cell and antibody responses *in vivo*

Mice were immunized subcutaneously with conjugate and controls on days 0 and 21. At one week post-boost (day 29), the strength of the endogenous $CD8^+$ T cell response was assessed based on the frequency of IFN-γ-secreting $CD8^+$ T cells in isolated splenocyte populations. Intracellular cytokine staining showed statistically elevated ($p<0.05$) levels of ova-specific $CD8^+$ T-cells (0.44 ± 0.09 % IFN-γ^+ of $CD8^+$) in mice immunized with the HP-PDB conjugate, as compared to controls (Figure 5a). Immunization with physical mixture produced a low but detectable response by intracellular cytokine staining (0.20 ± 0.03% IFN-γ^+ of $CD8^+$), suggesting a degree of co-uptake of antigen with polymer. Antibody production in immunized mice was analyzed from blood drawn on day 28. Elevated titers of antigen-specific IgG1 were observed with conjugate (610-fold) and mixture (425-fold) as compared to free protein and Ova-(HP-MMA) (Figure 5b; note that titers are plotted on a $\log_{10}$ axis). Polymer-containing groups also enhanced IgG2c titers relative to antigen alone (630- and 170-fold for conjugate and mixture respectively). Inactive conjugate generated no detectable IgG2c response (titer ≤ 2).

4. Discussion

Previous studies with pH-responsive polymers and polymeric micelles have demonstrated that carriers with endosomal-releasing activity can increase antigen-specific $CD8^+$ T-cell responses. Herein we evaluated a related pH-responsive micelle platform, which exploits a neutral corona-forming segment previously found to impart a favorable toxicity profile [18], for antigen delivery. The dynamics of intracellular trafficking and exocytosis were quantitated for the first time with this polymeric micelle system. These studies demonstrated the benefits of direct antigen conjugation and the role of the pH-responsive segment in promoting intracellular antigen accumulation. Enhancements in antigen uptake and intracellular retention (reduced exocytosis) were only observed when antigen was directly coupled to the membrane-destabilizing carrier. Improved uptake of active conjugates relative to the inactive conjugates was likely due to electrostatic interactions between some surface-exposed DMAEMA residues and the negatively charged cellular membrane.

Lower exocytosis rates could in part be due to polymer-mediated retardation of vesicle-vesicle fusion, which may delay intracellular antigen processing. Using subcellular fractionation in rat liver cells, Richardson *et al* previously observed that linear, cationic poly(amidoamine) gene delivery carriers transiently accumulated in vesicles with increased

buoyant density, indicative of inhibition of entry into the late endosomal-lysosomal organelle [43]. Additionally, active micelles may contribute to compartmental pH buffering, slowing the acidification of endosomes which inhibits their fusion and maturation [44]. Nanoparticle-induced pH buffering of intracellular compartments was previously observed by Hirosue *et al* in bone marrow derived dendritic cells treated with poly(propylene) sulfide nanoparticles [24].

The overall result of enhanced intracellular antigen presence on MHC-I presentation was evaluated in an *in vitro* cross-presentation assay. Even when normalized to uptake, the active carrier afforded a substantial advantage over free ova and inactive carrier at driving antigen cross-presentation. This could be attributed to the combined effects of reduced exocytosis, increased cytosolic delivery, and longer residence time in vesicular compartments which in some cases can also cross-present antigen [3]. Though an equal amount of antigen was internalized initially, the carrier aided in sustained payload delivery to the cell cytosol, thereby likely allowing for prolonged antigen presentation to T cells [5]. While not explored further here, enhancements in antigen cross-presentation may also in part be due to the formation of more stable MHC I-peptide complexes with extended half-lives, an effect which has been associated with inflammatory stimuli that may here be polymer-mediated [45].

Consistent with previous findings [10,40,46], polymeric micelles were shown to fall into a size range favorable for accessing DCs and macrophages in the draining lymph nodes. Interestingly, physical mixture of ova and polymer displayed uptake patterns similar to free ova at 90 min, but unlike free protein maintained some cell localization after 24 h. It is possible that the polymer creates a “depot effect” at the injection site, retaining a cohort of antigen long enough to be picked up by skin-resident APCs. While the non-pH-responsive particles are also in a favorable size range for lymphatic transport, the decrease in signal relative to the active formulation is likely due to marked differences in cellular uptake and intracellular residence times, as was observed *in vitro*.

As was previously demonstrated with related unimeric polymer-antigen conjugates and a cationic diblock polymer micelle, this new HPMA-based neutral corona micelle significantly elevated cellular and humoral immune responses. A control polymer micelle with a polyMMA core-forming segment was compared as a non-pH-responsive control. This carrier did not enhance cross-presentation in the B3Z assay, was not retained in draining lymph node APCs, and finally did not induce significant $CD8^+$ T-cell or antibody responses. These results underline the importance of the pH-responsive, membrane destabilizing block to this carrier system. Interestingly, the physical mixture induced modest levels of IFN-γ^+ $CD8^+$ T cells, indicating that co-injection of ova and polymer may result in low levels of co-uptake by tissue resident APCs, or combined transport to the lymph node APC population. It may also be possible that the pH-responsive segment has additional inflammatory and adjuvanting effects. Consistent with this possibility, the pH-responsive HP-PDB micelle induced a preferential IgG1 > IgG2 Th2-like antibody response. While not explored further in this work, these data suggest that the active carrier has intrinsic adjuvant properties which here may be enhancing Th2 $CD4^+$ T cell and B cell activity. Prior studies with other

synthetic vaccines have demonstrated that nanoparticles can exhibit adjuvant activities [47,48].

In summary, this work provides new mechanistic insights into how pH-responsive micelles can modulate intracellular antigen trafficking and thereby increase $CD8^+$ T cell responses. The membrane-interactive properties of the pH-responsive core block were shown to be essential for enhancing cytosolic delivery and cross-presentation of conjugated antigenic cargo *in vitro*, as well as for promoting superior antigen uptake by antigen presenting cells in the draining lymph nodes. Together, these effects significantly enhanced antigen-specific $CD8^+$ T cell responses *in vivo*. This versatile platform can be extended for use with other disulfide-linked antigens as well as adjuvants, affording the benefits of co-delivering antigen and immunostimulatory agent on a single particle.

Supplementary Material

Refer to Web version on PubMed Central for supplementary material.

Acknowledgments

The authors would like to thank D. Chiu and J. Shi (University of Washington Department of Bioengineering) for technical expertise, and M. Moutaftsi (Bill and Melinda Gates Foundation) for insightful discussions. This work was supported by the Science and Industry Endowment Fund of Australia, the National Institutes of Health (R01EB002991 and R21EB014572), the Washington State Life Science Discovery Fund (Grant No. 2496490), the National Science Foundation Graduate Research Fellowship under Grant DGE-1256082 (S.K.), the Irvington Institute Fellowship Program of the Cancer Research Institute (J.T.W.), the Mary Gates Undergraduate Research Fellowship (G.I.P.), and the University of Washington Medical Scientist Training Program (GM007266, H.B.K.)

References

1. Swartz MA, Hirosue S, Hubbell JA. Engineering approaches to immunotherapy. Sci Transl Med. 2012; 4:148rv9–148rv9.
2. Hubbell JA, Thomas SN, Swartz MA. Materials engineering for immunomodulation. Nature. 2009; 462:449–60. [PubMed: 19940915]
3. De Temmerman ML, Rejman J, Demeester J, Irvine DJ, Gander B, De Smedt SC. Particulate vaccines: on the quest for optimal delivery and immune response. Drug Discov Today. 2011; 16:569–82. [PubMed: 21570475]
4. Flanary S, Hoffman AS, Stayton PS. Antigen delivery with poly (propylacrylic acid) conjugation enhances MHC-1 presentation and T-Cell activation. Bioconjug Chem. 2009; 20:241–248. [PubMed: 19125614]
5. Shen H, Ackerman AL, Cody V, Giodini A, Hinson ER, Cresswell P, et al. Enhanced and prolonged cross-presentation following endosomal escape of exogenous antigens encapsulated in biodegradable nanoparticles. Immunology. 2006; 117:78–88. [PubMed: 16423043]
6. Smith DM, Simon JK, Baker JR. Applications of nanotechnology for immunology. Nat Rev Immunol. 2013; 13:592–605. [PubMed: 23883969]
7. Kourtis IC, Hirosue S, De Titta A, Kontos S, Stegmann T, Hubbell JA, et al. Peripherally administered nanoparticles target monocytic myeloid cells, secondary lymphoid organs and tumors in mice. PLoS One. 2013; 8:e61646. [PubMed: 23626707]
8. Akagi T, Shima F, Akashi M. Intracellular degradation and distribution of protein-encapsulated amphiphilic poly(amino acid) nanoparticles. Biomaterials. 2011; 32:4959–67. [PubMed: 21482432]
9. Wilson JT, Keller S, Manganiello MJ, Cheng C, Lee CC, Opara C, et al. pH-Responsive nanoparticle vaccines for dual-delivery of antigens and immunostimulatory oligonucleotides. ACS Nano. 2013; 7:3912–25. [PubMed: 23590591]

10. Eby JK, Dane KY, O'Neil CP, Hirosue S, Swartz MA, Hubbell JA. Polymer micelles with pyridyl disulfide-coupled antigen travel through lymphatics and show enhanced cellular responses following immunization. Acta Biomater. 2012; 8:3210–7. [PubMed: 22698945]
11. Jik Y, James E, Shastri N, Fréchet JMJ, Kwon YJ, Jamest E, et al. In vivo Targeting of Dendritic Cells for Activation of Cellular Immunity Using Vaccine Carriers Based on pH-Responsive Microparticles. PNAS. 2012; 102:18264–18268.
12. Moon JJ, Suh H, Bershteyn A, Stephan MT, Liu H, Huang B, et al. Interbilayer-crosslinked multilamellar vesicles as synthetic vaccines for potent humoral and cellular immune responses. Nat Med. 2011; 10:243–251.
13. Yuba E, Kojima C, Harada A, Tana, Watarai S, Kono K. pH-Sensitive fusogenic polymer-modified liposomes as a carrier of antigenic proteins for activation of cellular immunity. Biomaterials. 2010; 31:943–51. [PubMed: 19850335]
14. Zhang J, Wu L, Meng F, Wang Z, Deng C, Liu H, et al. pH and reduction dual-bioresponsive polymersomes for efficient intracellular protein delivery. Langmuir. 2012; 28:2056–65. [PubMed: 22188099]
15. Stano A, Scott EA, Dane KY, Swartz MA, Hubbell JA. Tunable T cell immunity towards a protein antigen using polymersomes vs. solid-core nanoparticles. Biomaterials. 2013:2–9. [PubMed: 24120043]
16. Kaminskas LM, Porter CJH. Targeting the lymphatics using dendritic polymers (dendrimers). Adv Drug Deliv Rev. 2011; 63:890–900. [PubMed: 21683746]
17. Foster S, Duvall CL, Crownover EF, Hoffman AS, Stayton PS. Intracellular delivery of a protein antigen with an endosomal-releasing polymer enhances CD8 T-Cell production and prophylactic vaccine efficacy. Bioconjug Chem. 2010; 21:2205–12. [PubMed: 21043513]
18. Lundy BB, Convertine A, Miteva M, Stayton PS. Neutral polymeric micelles for RNA delivery. Bioconjug Chem. 2013; 24:398–407. [PubMed: 23360541]
19. Convertine AJ, Diab C, Prieve M, Paschal A, Hoffman AS, Johnson PH, et al. pH-responsive polymeric micelle carriers for siRNA drugs. Biomacromolecules. 2010; 11:2904–2911. [PubMed: 20886830]
20. Skehel JJ, Wiley DC. Receptor binding and membrane fusion in virus entry: The influenza hemagglutinin. Annu Rev Biochem. 2000; 12:531–69. [PubMed: 10966468]
21. Scales CW, Vasilieva YA, Convertine AJ, Lowe AB, McCormick CL. Direct, controlled synthesis of the nonimmunogenic, hydrophilic polymer, poly(N-(2-hydroxypropyl)methacrylamide) via RAFT in aqueous media. Biomacromolecules. 2005; 6:1846–50. [PubMed: 16004419]
22. Convertine AJ, Benoit DSW, Duvall CL, Hoffman AS, Stayton PS. Development of a novel endosomolytic diblock copolymer for siRNA delivery. J Control Release. 2009; 133:221–9. [PubMed: 18973780]
23. Nembrini C, Stano A, Dane KY, Ballester M, van der Vlies AJ, Marsland BJ, et al. Nanoparticle conjugation of antigen enhances cytotoxic T-cell responses in pulmonary vaccination. PNAS. 2011; 108:E989–97. [PubMed: 21969597]
24. Hirosue S, Kourtis IC, van der Vlies AJ, Hubbell JA, Swartz MA. Antigen delivery to dendritic cells by poly(propylene sulfide) nanoparticles with disulfide conjugated peptides: cross-presentation and T cell activation. Vaccine. 2010; 28:7897–906. [PubMed: 20934457]
25. Duvall CL, Convertine AJ, Benoit DSW, Hoffman AS, Stayton PS. Intracellular delivery of a proapoptotic peptide via conjugation to a RAFT synthesized endosomolytic polymer. Mol Pharm. 2010; 7:468–76. [PubMed: 19968323]
26. Kim J, Tirrell DA. Synthesis of well-defined poly (2-ethylacrylic acid). Macromolecules. 1999; 32:945–948.
27. Murthy N, Robichaud JR, Tirrell DA, Stayton PS, Hoffman AS. The design and synthesis of polymers for eukaryotic membrane disruption. J Control Release. 1999; 61:137–43. [PubMed: 10469910]
28. Karttunen J, Sanderson S, Shastri N. Detection of rare antigen-presenting cells by the lacZ T-cell activation assay suggests an expression cloning strategy for T-cell antigens. PNAS. 1992; 89:6020–4. [PubMed: 1378619]

29. Shi J, Chou B, Choi JL, Ta A, Pun SH. Investigation of polyethylenimine/DNA polyplex transfection to cultured cells using radiolabeling and subcellular fractionation methods. Mol Pharm. 2013
30. Brito LA, Singh M. Acceptable levels of endotoxin in vaccine formulations during preclinical research. J Pharm Sci. 2011; 100:34–37. [PubMed: 20575063]
31. Chiefari J, Chong YKB, Ercole F, Kristina J, Jeffery J, Le TPT, et al. Living free-radical polymerization by reversible addition - fragmentation chain transfer: the RAFT process. Macromolecules. 1998; 9297:5559–5562.
32. Moad G, Rizzardo E, Thang SH. Living radical polymerization by the RAFT process. Aust J Chem. 2005; 58:379.
33. Szablan Z, Toy AAH, Terrenoire A, Davis TP, Barner-Kowollik C. Living free-radical polymerization of sterically hindered monomers: improving the understanding of 1,1-disubstituted monomer systems. J Polym Sci Part A Polym Chem. 2006; 44:3692–3710.
34. Szablan Z, Toy AA, Davis TP, Hao X, Stenzel MH, Barner-Kowollik C. Reversible addition fragmentation chain transfer polymerization of sterically hindered monomers: Toward well-defined rod/coil architectures. J Polym Sci Part A Polym Chem. 2004; 42:2432–2443.
35. Seib FP, Jones AT, Duncan R. Establishment of subcellular fractionation techniques to monitor the intracellular fate of polymer therapeutics I. Differential centrifugation fractionation B16F10 cells and use to study the intracellular fate of HPMA copolymer-doxorubicin. J Drug Target. 2006; 14:375–90. [PubMed: 17092838]
36. Wendeler M, Sandhoff K. Hexosaminidase assays. Glycoconj J. 2009; 26:945–52. [PubMed: 18473163]
37. Gorvel JP, Chavrier P, Zerial M, Gruenberg J. Rab5 controls early endosome fusion in vitro. Cell. 1991; 64:915–925. [PubMed: 1900457]
38. Eskelinen E, Illert AL, Tanaka Y, Blanz J, Von Figura K, Saftig P, et al. Role of LAMP-2 in lysosome biogenesis and autophagy. Mol Biol Cell. 2002; 13:3355–3368. [PubMed: 12221139]
39. Reddy ST, van der Vlies AJ, Simeoni E, Angeli V, Randolph GJ, O'Neil CP, et al. Exploiting lymphatic transport and complement activation in nanoparticle vaccines. Nat Biotechnol. 2007; 25:1159–64. [PubMed: 17873867]
40. Reddy ST, Rehor A, Schmoekel HG, Hubbell JA, Swartz MA. In vivo targeting of dendritic cells in lymph nodes with poly(propylene sulfide) nanoparticles. J Control Release. 2006; 112:26–34. [PubMed: 16529839]
41. Salomon B, Cohen JL, Masurier C, Klatzmann D. Three populations of mouse lymph node dendritic cells with different origins and dynamics. J Immunol. 1998; 160:708–17. [PubMed: 9551906]
42. Macatonia SE, Knight SC, Edwards AJ, Griffiths S, Fryer P. Localization of antigen on lymph node dendritic cells after exposure to the contact sensitizer fluorescein isothiocyanate. J Exp Med. 1987; 166:1654–1667. [PubMed: 3119761]
43. Richardson SCW, Pattrick NG, Lavignac N, Ferruti P, Duncan R. Intracellular fate of bioresponsive poly(amidoamine)s in vitro and in vivo. J Control Release. 2010; 142:78–88. [PubMed: 19822175]
44. Johnson LS, Dunn KW, Pytowski B, McGraw TE. Endosome acidification and receptor trafficking: bafilomycin A1 slows receptor externalization by a mechanism involving the receptor's internalization motif. Mol Biol Cell. 1993; 4:1251–66. [PubMed: 8167408]
45. Crespo MI, Zacca ER, Núñez NG, Ranocchia RP, Maccioni M, Maletto BA, et al. TLR7 triggering with polyuridylic acid promotes cross-presentation in CD8α+ conventional dendritic cells by enhancing antigen preservation and MHC class I antigen permanence on the dendritic cell surface. J Immunol. 2013; 190:948–60. [PubMed: 23284054]
46. Manolova V, Flace A, Bauer M, Schwarz K, Saudan P, Bachmann MF. Nanoparticles target distinct dendritic cell populations according to their size. Eur J Immunol. 2008; 38:1404–13. [PubMed: 18389478]
47. Wegmann F, Gartlan KH, Harandi AM, Brinckmann SA, Coccia M, Hillson WR, et al. Polyethyleneimine is a potent mucosal adjuvant for viral glycoprotein antigens. Nat Biotechnol. 2012:1–8. [PubMed: 22231070]

48. Akagi T, Baba M, Akashi M. Biodegradable nanoparticles as vaccine adjuvants and delivery systems: regulation of immune responses by nanoparticle-based vaccines. Adv Polym Sci. 2012; 247:31–64.

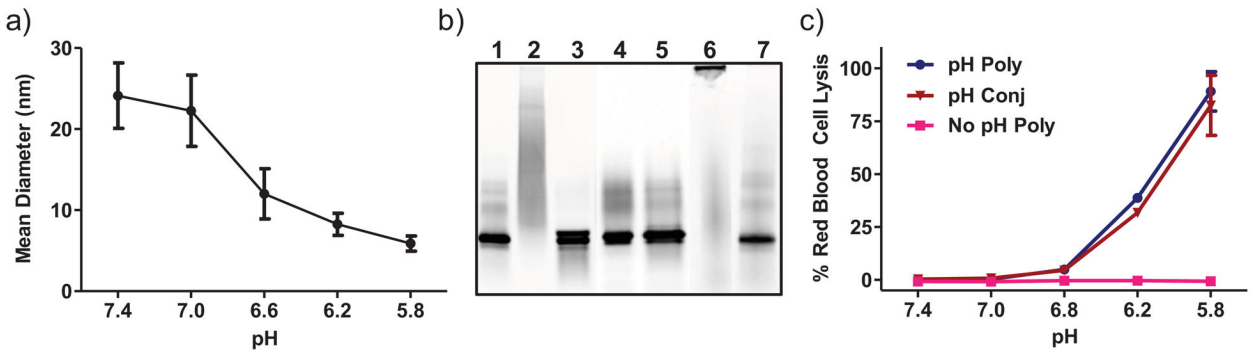

Figure 1. Conjugation of ova to polymer carrier via a reducible disulfide linkage

a) pH-responsive carrier transitions from micelle to unimer as a function of pH. HP-PDB was incubated in phosphate buffers ranging from pH 7.4 (physiologic) to 5.8 (endosomal) and particle size analyzed by dynamic light scattering, 1 mg/mL polymer. Data are from a single experiment run in triplicate with error bars representing the standard deviation. **b)** Fluorescence image of non-reducing SDS-PAGE validating protein-polymer conjugation via a reducible disulfide linkage, 2.8 μg ova-AF488/lane: native ova (Ova) (1), pH-responsive conjugate at 20:1 polymer:ova molar ratio [Ova-(HP-PDB)] (2), conjugate + 20mM TCEP (3), physical mixture of ova and polymer [Ova+(H-PDB)] (4), mixture + 20mM TCEP (5), non pH-responsive control conjugate [Ova-(HP-MMA)] (6), non pH-responsive control conjugate + 20mM TCEP (7). **c)** Hemolytic activity of diblock copolymer with [Ova-(HP-PDB)] and without (HP-PDB) antigen conjugation, of mixture control polymer (H-PDB), and of non pH-responsive control polymer (HP-MMA), at a polymer concentration of 40 μg/mL. Values are normalized relative to a positive control, 1% v/v Triton X-100, and data represent a single experiment conducted in triplicate ± SD.

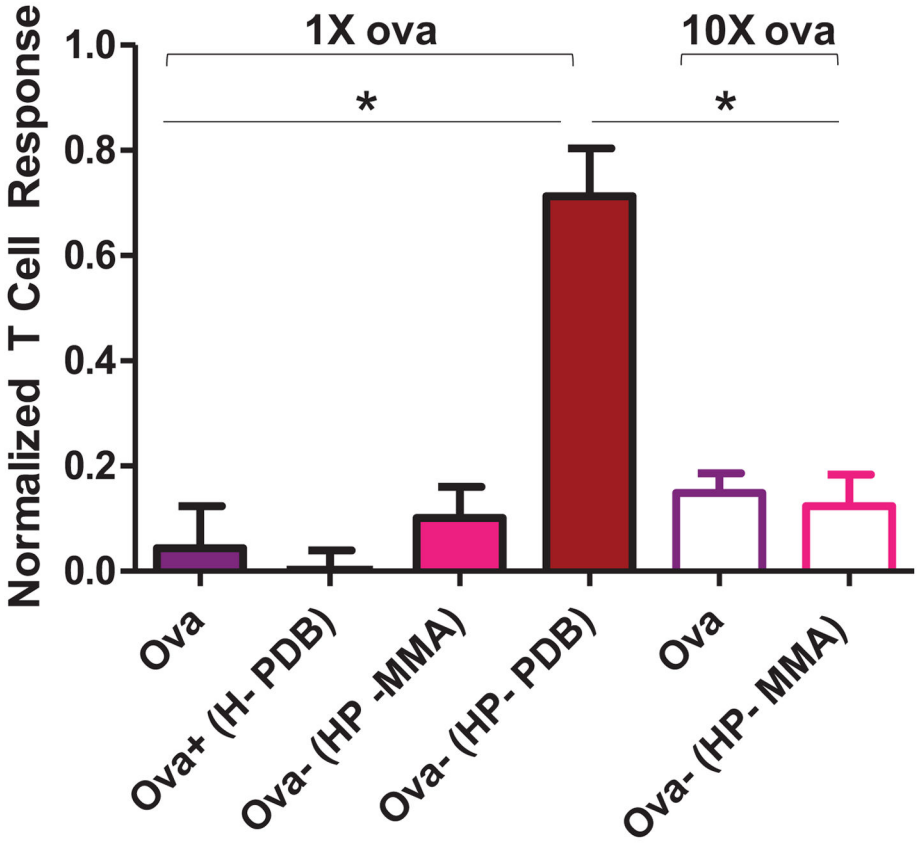

Figure 2. Antigen conjugation enhances CTL activation/MHC-I presentation *in vitro*

DC2.4 cells were stimulated with free protein, physical mixture, or conjugates (10 or 100 μg/mL ova) for 4 h and subsequently co-cultured with B3Z T-cells for 24 h. Cells were rinsed, incubated 24 h with lysis buffer containing chlorophenol red β-D-galactoside, and the absorbance of released chlorophenol red measured at 570 nm. Data represent a representative experiment performed in quadruplicate, mean ± SD. One-way ANOVA followed by Tukey's Multiple Comparison Test was used for statistical analysis, * = $p < 0.05$.

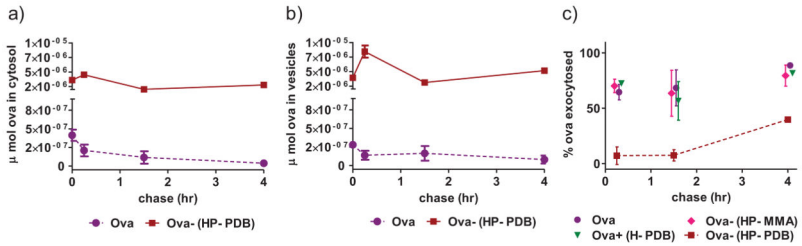

Figure 3. Conjugation enhances antigen accumulation in DC 2.4s

a,b) DC 2.4s were pulsed with ova or active conjugate (2.5 μg/mL ^{3}H-ova) for 4 h. After various chase periods cells were homogenized and cytosolic and vesicular components separated by ultracentrifugation. Ova content was determined by radioactivity measurements and is plotted in terms of μmol ova. Data represent n = 3 ± SD. **c)** DC2.4s were pulsed with treatment groups (2.5 μg/mL ^{3}H-ova) for 4 h. After various chase times cells were lysed to measure the intracellular radioactivity. Exocytosis of ^{3}H-ova represents the decrease in intracellular radioactivity in cells post chase relative to radioactivity in cell lysates after the 4 h pulse period. Data from a representative experiment conducted in triplicate ± SD is shown.

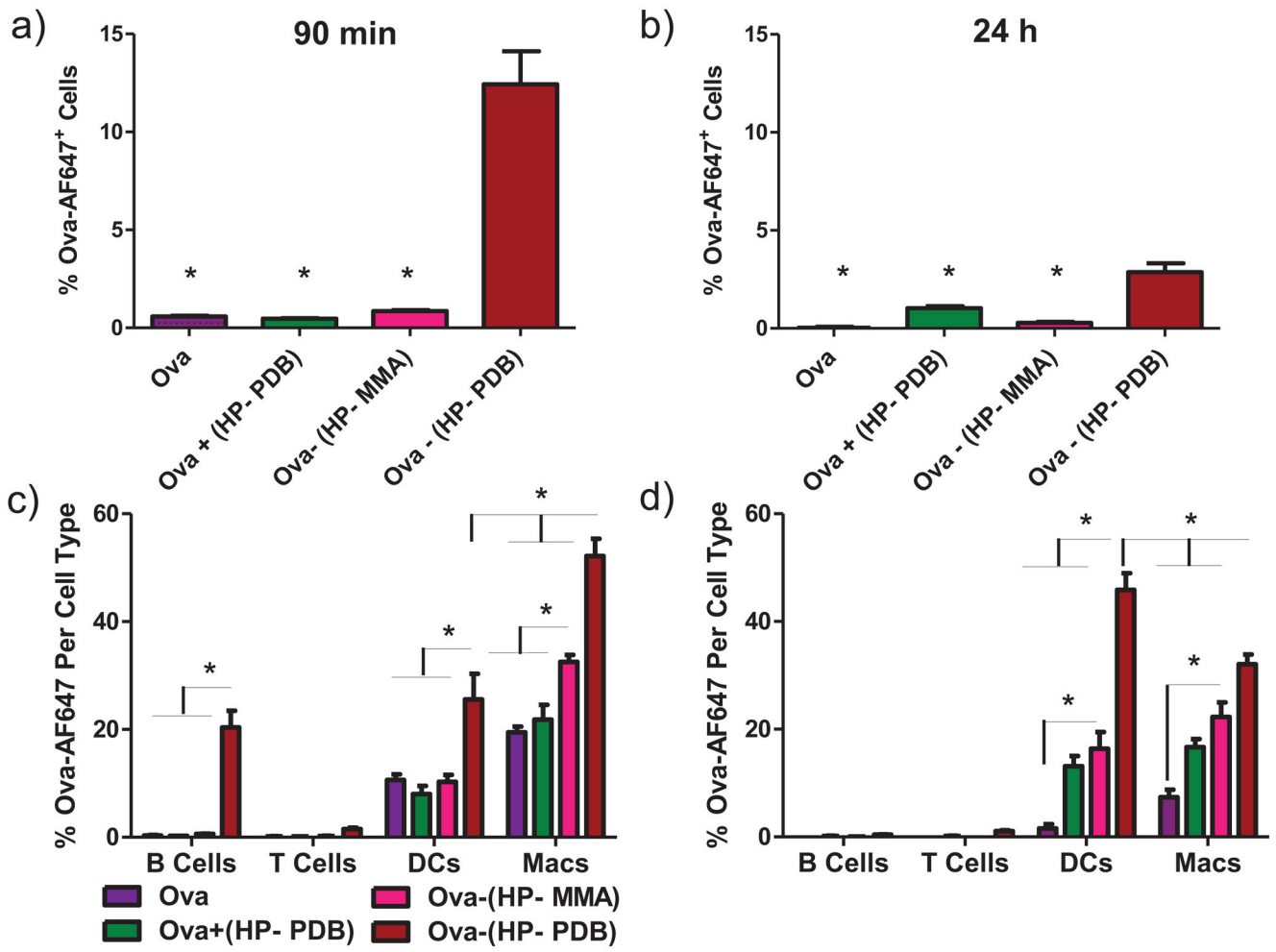

Figure 4. Conjugation enhances antigen delivery to lymph node APCs

C57Bl/6 mice were immunized with free ova, mixture, or conjugates in the dorsal part of the foot and draining popliteal lymph nodes isolated 90 min and 24 h post injection. **a,b)** Uptake of fluorescent ova in total lymphocyte populations as measured by flow cytometry. One-way ANOVA followed by Tukey's Multiple Comparison Test was used for statistical analysis at a level of $p < 0.05$ with * indicating significance as compared to Ova-(HP-PDB). **c,d)** Uptake of ova in individual lymphocyte cell subtypes. Data shown are from two independent experiments with n = 6 mice per group, mean ± SEM. * = $p < 0.05$, one-way ANOVA followed by Tukey's Multiple Comparison Test.

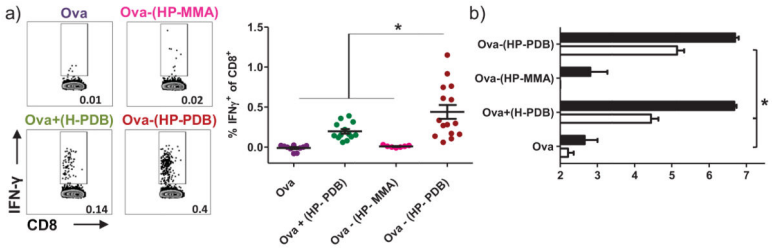

Figure 5. Conjugation enhances antigen-specific CD8$^+$ IFN-γ$^+$ T cell and antibody responses

Splenocytes were isolated on day 29 from mice immunized twice, 3 weeks apart, with free ova, physical mixture, and pH-responsive conjugate. **a)** Cells were plated and tested for IFN-γ *in vitro* recall responses by incubating with CD8$^+$ T cell epitope ova$_{257-264}$ (SINFEKL). CD8$^+$ T cells were identified by ICS based on CD8 expression, and the percentage of these cells expressing IFN-γ determined. Means ± SEM (n = 7–15) shown are pooled from three independent experiments. Representative flow cytometry dot plots of CD8$^+$ IFN-γ$^+$ T cells from individual mice. **b)** Ova-specific IgG1 (black bars) and IgG2c (white bars) antibody titres were measured on day 28 in sera from immunized mice. Data shown are pooled from four independent experiments and represent the mean of the reciprocal dilution ± SEM (n = 7–15). One-way ANOVA followed by Tukey's Multiple Comparison Test was used for all statistical analyses. *$p < 0.05$.

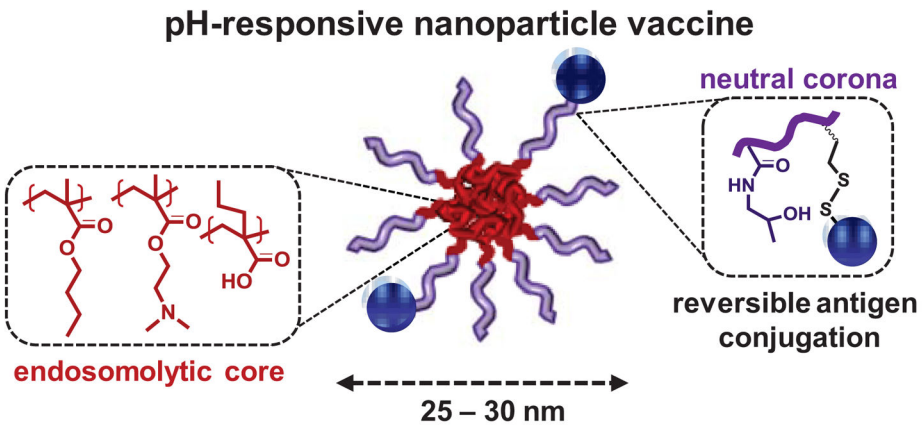

Scheme 1. Nanoparticle vaccine based on pH-responsive polymers for antigen delivery

Amphiphilic diblock copolymers were synthesized by controlled Reversible Addition-Fragmentation Chain Transfer (RAFT) polymerization and consist of a neutral, hydrophilic corona segment with pendant pyridyl disulfide groups for reversible antigen conjugation, and a hydrophobic, pH-responsive core that drives endosomal membrane destabilization. The carrier self-assembles into 25–30 nm micelles under aqueous conditions.